nature structural & molecular biology

© 2004 Nature Publishing Group http://www.nature.com/natstructmolbiol

Kinetic analysis of the RNAi enzyme complex

Benjamin Haley & Phillip D Zamore

The siRNA-directed ribonucleoprotein complex, RISC, catalyzes target RNA cleavage in the RNA interference pathway. Here, we show that siRNA-programmed RISC is a classical Michaelis-Menten enzyme in the presence of ATP. In the absence of ATP, the rate of multiple rounds of catalysis is limited by release of the cleaved products from the enzyme. Kinetic analysis suggests that different regions of the siRNA play distinct roles in the cycle of target recognition, cleavage, and product release. Bases near the siRNA 5′ end disproportionately contribute to target RNA-binding energy, whereas base pairs formed by the central and 3′ regions of the siRNA provide a helical geometry required for catalysis. Finally, the position of the scissile phosphate on the target RNA seems to be determined during RISC assembly, before the siRNA encounters its RNA target.

In the RNA interference (RNAi) pathway[1,2], 21-nucleotide (nt), double-stranded siRNAs guide the RISC[3–5] (RNA-induced silencing complex) to destroy its RNA target[6]. siRNA-directed RNAi has become an essential laboratory tool for reducing the expression of specific genes in mammalian cells[7], but the limits of siRNA specificity remain to be determined[8–11]. Some siRNAs can discriminate between mRNAs that differ by only a single nucleotide[7,9,12,13], but genome-wide assessments of siRNA specificity suggest that mRNAs with only partial complementarity to an siRNA can also be targeted for destruction[14]. Why some mismatches are tolerated, whereas others are not, remains poorly understood. One hypothesis is that the 5′ region of siRNAs and the related microRNAs (miRNAs) play a special role in target recognition, nucleating binding of RISC to the RNA target[15–17]. Alternatively, mismatched siRNA might recruit RISC to targets lacking complementarity to the 5′ region of the siRNA, but the geometry of such siRNA-target pairing is incompatible with target silencing.

To understand how the 5′, central and 3′ sequences of the siRNA guide strand function to direct target cleavage, we undertook a detailed *in vitro* kinetic analysis of a single siRNA sequence. Here, we show that RISC can cleave RNA targets with up to five contiguous mismatches at the siRNA 5′ end and nine mismatches at the siRNA 3′ end. Our data show that 5′ bases contribute disproportionately to target RNA binding, but do not play a role in determining the catalytic rate, k_{cat}. This finding resembles the earlier observations by Doench and Sharp that 5′ complementarity is essential for translational repression by siRNAs designed to act like animal miRNAs, which typically repress translation[18]. For siRNAs directing target cleavage, we find that the 3′ bases of the siRNA contribute much less than 5′ bases to the overall strength of binding, but instead help to establish the helical geometry required for RISC-mediated target cleavage, consistent with the view that catalysis by RISC requires a central A-form helix[19]. Finally, we show that when an siRNA fails to pair with the first three, four or five nucleotides of the target RNA, the phosphodiester bond severed in the target RNA is unchanged; for perfectly matched siRNA, RISC measures the site of cleavage from the siRNA 5′ end[2,9]. We conclude that the identity of the scissile phosphate is determined before the encounter of the RISC with its target RNA, perhaps because the RISC endonuclease is positioned with respect to the siRNA 5′ end during RISC assembly.

RESULTS

The siRNA-programmed RISC is an enzyme

RISC programmed with small RNA *in vivo* catalyzes the destruction of target RNA *in vitro* without consuming its small RNA guide[11,20]. To begin a kinetic analysis of RISC, we first confirmed that RISC programmed *in vitro* with siRNA is likewise a multiple-turnover enzyme. To engineer an RNAi reaction that contained a high substrate concentration relative to RISC, we used an siRNA in which the guide strand is identical to the *let-7* miRNA, but unlike the miRNA, the *let-7* siRNA is paired to an RNA strand that is antisense to *let-7*[20]. The *let-7* strand of this siRNA has a high intrinsic cleaving activity, but a reduced efficiency of incorporation into RISC (**Supplementary Fig. 1** online).

After incubating the *let-7* siRNA with *Drosophila melanogaster* embryo lysate in the presence of ATP, RISC assembly was inactivated by treatment with *N*-ethyl maleimide (NEM), and the amount of RISC generated was measured using the previously described tethered 2′-*O*-methyl oligonucleotide assay[21,22] (**Supplementary Fig. 1** online). The amount of *let-7*-programmed RISC increased with increasing siRNA concentration, until the assembly reaction began to saturate at ~50 nM, reaching an asymptote between 3 and 4 nM RISC. Using 0.6 nM RISC, we observed >50 cycles of target recognition and cleavage per enzyme complex (data not shown), confirming that siRNA-programmed RISC is a multiple-turnover enzyme.

Multiple turnover is limited by product release

Next, we evaluated the kinetics of siRNA-directed target cleavage in the presence and absence of ATP (–ATP; **Fig. 1**). RISC was assembled

Department of Biochemistry and Molecular Pharmacology, University of Massachusetts Medical School, Worcester, Massachusetts 01605, USA. Correspondence should be addressed to P.Z. (phillip.zamore@umassmed.edu).

Published online 30 May 2004; doi:10.1038/nsmb780

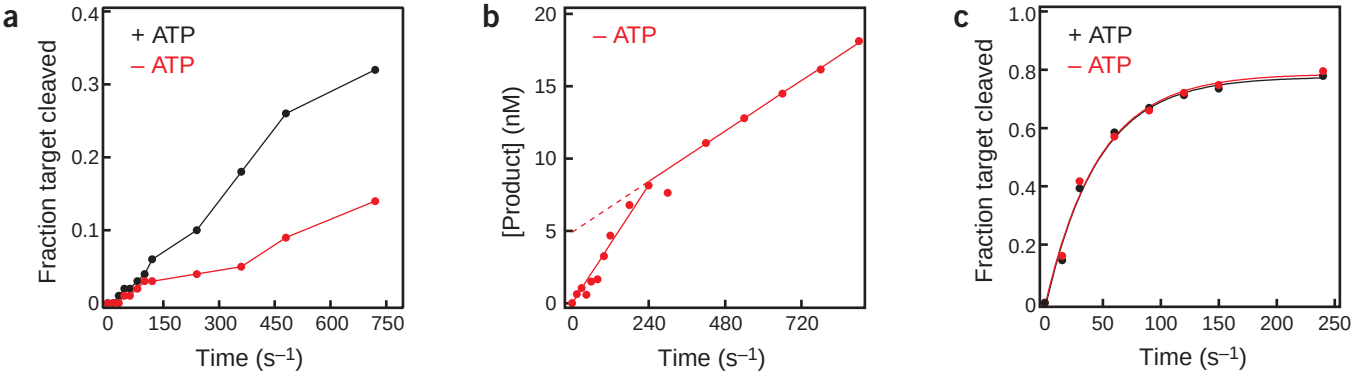

Figure 1 Product release limits the rate of catalysis by RISC. (**a**) ATP stimulates multiple rounds of RISC cleavage of the RNA target. siRNA was incubated with ATP in *D. melanogaster* embryo lysate, and then NEM was added to quench RISC assembly and to disable the ATP-regenerating system. The energy-regenerating system was either restored by adding additional creatine kinase (+ATP) or the reaction was ATP-depleted by adding hexokinase and glucose (–ATP). The target RNA concentration was 49 nM and the concentration of RISC was ~4 nM. The siRNA sequence is given in **Supplementary Figure 3** online. (**b**) In the absence of ATP, cleavage by RISC produces a pre-steady-state burst equal, within error, to the concentration of active RISC. The target concentration was 110 nM and the RISC concentration was ~4 nM. (**c**) Catalysis by RISC is not enhanced by ATP under single-turnover conditions. RISC was present in about eight-fold excess over target. Each data point represents the average of two trials.

© 2004 Nature Publishing Group http://www.nature.com/natstructmolbiol

in the presence of ATP (+ATP), and then the energy-regenerating enzyme creatine kinase was inactivated with NEM, and ATP was depleted by the addition of hexokinase and glucose (–ATP conditions). For +ATP measurements, we added back creatine kinase to the reaction after NEM treatment, and omitted the hexokinase treatment. We observed a faster rate of cleavage in the presence of ATP than in its absence. This difference was only apparent late in the reaction time course, suggesting that the ATP-dependent rate of cleavage was faster than the ATP-independent rate only at steady state (**Fig. 1a**). We therefore repeated the analysis in more detail (**Fig. 1b**). In the absence of ATP, we observed a burst of cleaved product early in the reaction, followed by an approximately four-fold slower rate of target cleavage. No burst was observed in the presence of ATP (**Fig. 1a**). If the burst corresponds to a single turnover of enzyme, then extrapolation of the slower steady-state rate back to the *y*-axis should give the amount of active enzyme in the reaction. The *y*-intercept at the start of the reaction for the steady-state rate was 4.9 nM, in good agreement with the amount of RISC estimated using the tethered 2′-*O*-methyl oligonucleotide assay (~4 nM; **Fig. 1b**).

In principle, ATP could enhance target recognition by RISC, promote a rearrangement of the RISC–target complex to an active form, facilitate cleavage itself, promote the release of the cleavage products from the siRNA guide strand, or help restore RISC to a catalytically competent state after product release. All of these steps, except product release and restoration to catalytic competence, should affect the rate of both multiple- and single-turnover reactions. Therefore, we next analyzed the rate of reaction in the presence and in the absence of ATP under conditions in which RISC was in excess over the RNA target. At early times under these conditions, the reaction rate should reflect only single-turnover cleavage events, in which events after cleavage do not determine the rate of reaction. Using single-turnover reaction conditions, we observed identical rates of RISC-mediated cleavage in the presence and absence of ATP (**Fig. 1c**). Thus, ATP must enhance a step that occurs only when each RISC catalyzes multiple cycles of target cleavage.

If product release is rate-determining for multiple-turnover catalysis by RISC in the absence, but not the presence, of ATP, then modifications that weaken the strength of pairing to the target RNA might enhance product release, but would not be expected to accelerate the return of the RISC to a catalytically competent state. We incorporated mismatches between the siRNA and its RNA target at the 3′ end of the siRNA guide strand and designed the siRNAs to be functionally asymmetric, ensuring efficient and predictable incorporation of the *let-7* strand into RISC (**Fig. 2a**)[22]. We compared the reaction velocity under conditions of substrate excess in the presence and absence of ATP for siRNAs with zero to four mismatches between the guide strand 3′ end and the RNA target. Cleavage was measured from 100 to 540 s, when >90% of the target remained uncleaved, ensuring that the multiple-turnover reaction was at steady state. Even a single 3′ mismatch between the siRNA and its target increased the –ATP rate, relative to the +ATP rate, and siRNAs with two or more mismatches showed no substantial difference in rate between the presence and absence of ATP (**Fig. 2b**). We conclude that in the absence of ATP, product release is the rate-determining step for siRNAs fully matched to their RNA targets.

siRNA-target complementarity and RISC function

Mismatches between the siRNA and its target facilitate product release, but not without cost: the rate of reaction, irrespective of ATP concentration, decreases with each additional 3′ mismatch. When the concentration of RISC was ~16–80-fold greater than the target RNA concentration, each additional mismatch between the 3′ end of the siRNA guide strand and the RNA target further slowed the reaction (**Fig. 2c,d**). Under conditions of substrate excess, the effect of mismatches between the 3′ end of the siRNA guide strand and its RNA target was more marked (**Fig. 3a**): the rate of cleavage slowed ~20% for each additional mismatch. To test the limits of the tolerance of RISC for 3′ mismatches, we analyzed cleavage under modest (8-fold, **Fig. 3b**) and vast (~80-fold, **Figs. 3c** and **Fig. 4**) enzyme excess over target RNA. Notably, cleavage was detected for siRNAs with as many as nine 3′ mismatches to the RNA target (**Figs. 3c** and **4c**), but only after 24 h incubation. No cleavage was detected for an siRNA with ten 3′ mismatches to the RNA target (**Fig. 3c**).

Linsley and colleagues have proposed siRNA-directed downregulation of an mRNA with as few as 11 contiguous bases complementary to the siRNA guide strand[14]. In that study, the mRNA target paired with positions 2–5 and 7–17 of the siRNA guide strand, but was mismatched at positions 1 and 6 of the siRNA. We find that up to five mismatched bases are tolerated between the 5′ end of the siRNA and its

© 2004 Nature Publishing Group http://www.nature.com/natstructmolbiol

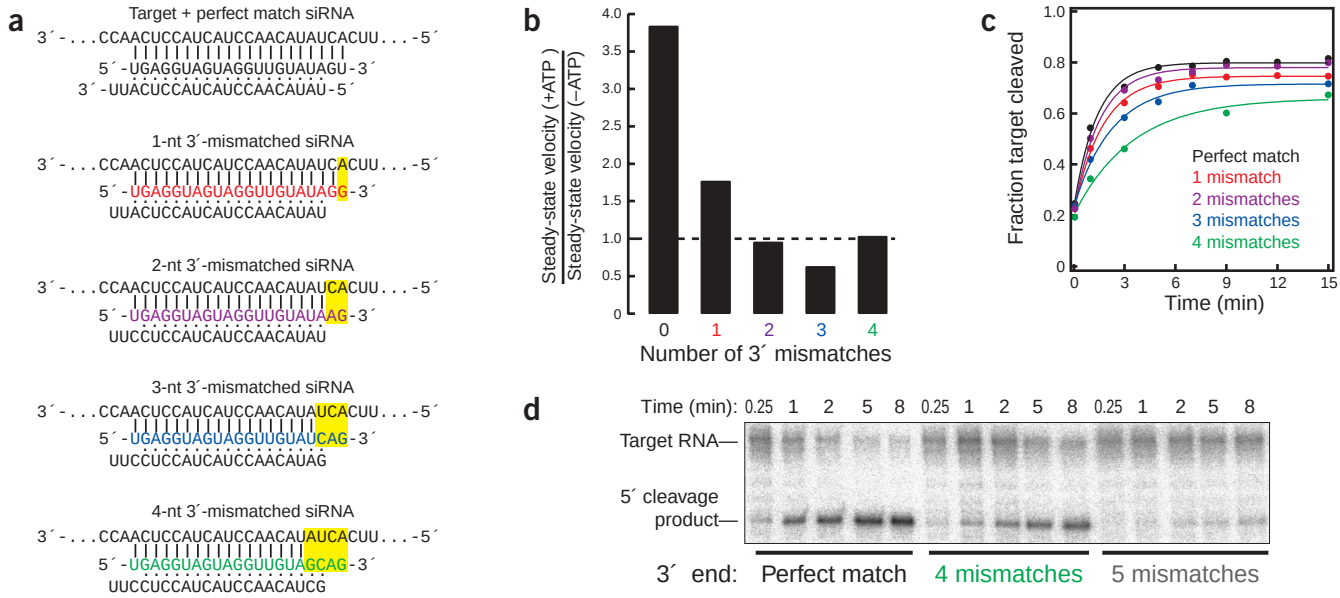

Figure 2 In the absence of ATP, mismatches between the 3′ end of the siRNA guide strand and the target RNA facilitate product release, but reduce the rate of target cleavage. (**a**) Representative siRNA sequences aligned with the target sequence. The siRNA guide strand is colored (5′→3′) and the mismatch with the target site is highlighted yellow. A complete list of siRNA sequences appears in **Supplementary Figure 3** online. (**b**) The steady-state rate of cleavage in the presence and absence of ATP was determined for siRNAs with zero to four 3′ mismatches with the target site. The target RNA concentration was 49 nM and the concentration of RISC was either ~4 nM (no mismatches) or ~6 nM (1–4 mismatches). The steady-state velocity with ATP, relative to the velocity without ATP, is shown for each siRNA. (**c**) Time course of cleavage for perfectly matched (~16-fold excess of RISC relative to target) and mismatched (~80-fold excess of RISC) siRNA. (**d**) Data representative of those used in the analysis in **c** for target cleavage directed by siRNAs with zero, four and five 3′ mismatches.

RNA target (**Fig. 4a,b**). No cleavage was detected for siRNAs with six, seven or eight 5′ mismatches to the target, even after 24 h incubation. The siRNA bearing eight mismatches between its 5′ end and the *let-7* complementary target was fully active when eight compensatory mutations were introduced into the *let-7*-binding site (**Figs. 3c** and **4b**), demonstrating that mutation of the siRNA was not the cause of its inactivity against the mismatched target. Similarly, when eight mismatches with the 3′ or 5′ end of the siRNA were created by changing the sequence of the RNA target, we detected target RNA cleavage when the target contained eight mismatches with the siRNA 3′ end, but not with the 5′ end (**Fig. 4b,c**).

To begin to estimate the minimal number of base pairs between the siRNA and its target that permit detectable cleavage by RISC at 24 h incubation, we combined seven, eight or nine 3′ mismatches with increasing numbers of 5′ mismatches (**Fig. 4c**). Cleavage was detected for as many as nine 3′ mismatches. But no detectable cleavage occurred when seven, eight or nine 3′ mismatches were combined with two or more 5′ mismatches. In contrast, a single 5′ mismatch (p1) enhanced target cleavage directed by all three 3′ mismatched siRNAs. Only 6% of the target RNA was cleaved after 24 h when the siRNA contained nine contiguous 3′ mismatches with the target RNA, but 10% was cleaved when the siRNA contained both nine 3′ mismatches and a single (p1)

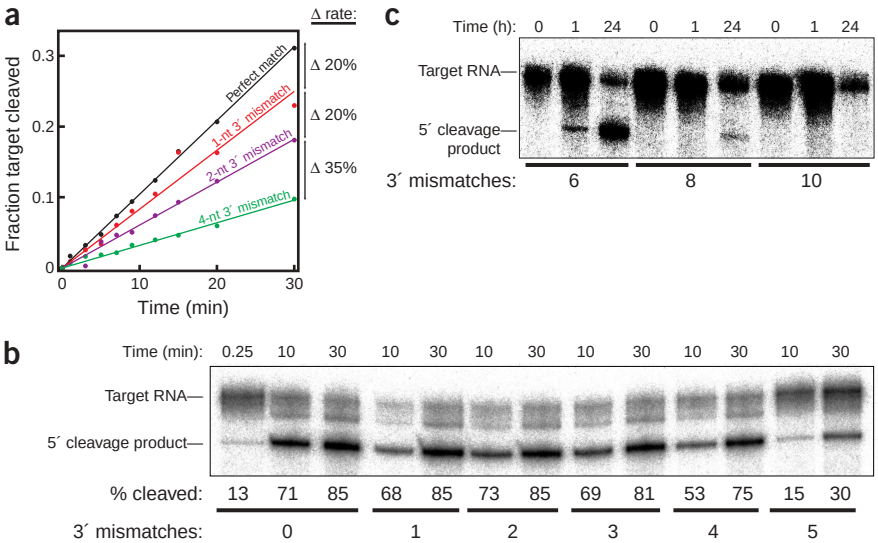

Figure 3 Tolerance of RISC for 3′ mismatches. (**a**) Each additional 3′ mismatch further reduced the rate of cleavage by RISC. The steady-state rates of cleavage were determined for siRNA with zero, one, two and four mismatches under multiple-turnover conditions (~49 nM target mRNA and ~4–6 nM RISC). (**b**) Analysis of siRNAs bearing zero to five 3′ mismatches with the target RNA under conditions of slight enzyme excess (about two-fold more RISC than target). siRNA sequences used in **a** and **b** are shown in **Figure 2a** and **Supplementary Figure 3** online. (**c**) Extended endpoint analysis of RISC cleavage under conditions of ~80-fold enzyme excess reveals that cleavage can occur for siRNAs with as many as eight mismatches to the target RNA. Note the different time scales in **c** versus **b**. All reactions were under standard *in vitro* RNAi (+ATP) conditions.

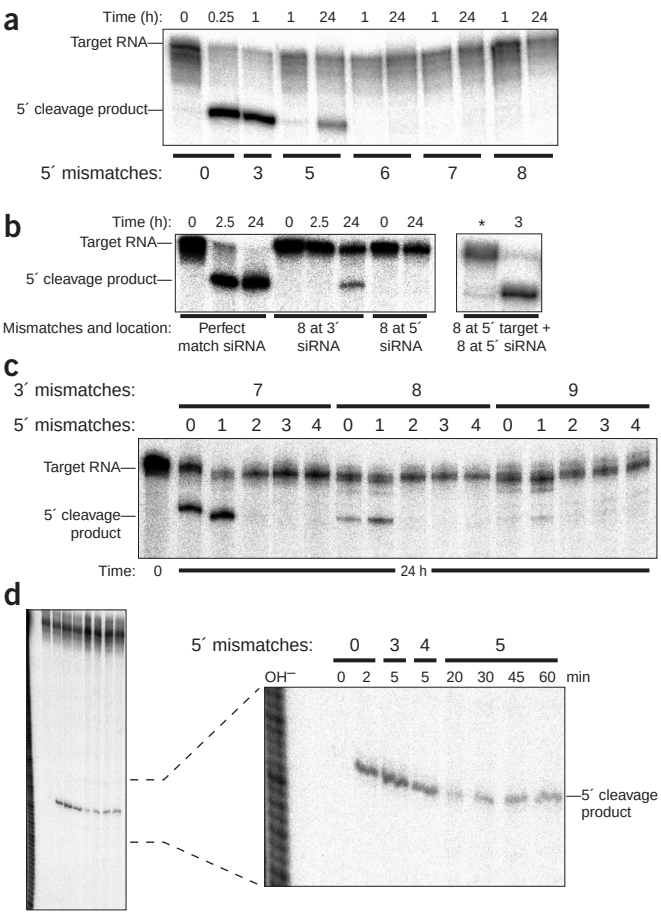

Figure 4 Limited tolerance of RISC for 5′ mismatches. (**a**) RISC cleavage was analyzed as in **Figure 3c** using 5′-mismatched siRNAs whose sequences are given in **Supplementary Figure 3** online. The target RNA was the same for all siRNAs. (**b**) RISC cleavage was analyzed using a single siRNA sequence. Mismatches were created by altering the sequence of the target RNA. For the target containing compensatory mutations, the target concentration was 0.25 nM and the siRNA concentration was ~20 nM; RISC concentration was not determined. Asterisk, 15-s time point. (**c**) RISC cleavage was analyzed by incubating 50 nM siRNA with 0.5 nM target RNA. 3′ mismatches were created by modifying the target sequence, and 5′ mismatches by changing the siRNA. Target and siRNA sequences are given in **Supplementary Figure 3** online. (**d**) Perfectly base-paired and 5′-mismatched siRNAs direct cleavage at the same phosphodiester bond. Cleavage reactions were carried out with ~20 nM RISC generated from 50 nM siRNA and 0.5 nM target RNA and analyzed on 8% (w/v) denaturing PAGE. The lengths of the target mRNA and 5′ cleavage product were 182 nt and 148 nt, respectively. After RISC was assembled, the extract was treated with NEM to inactivate nucleases[43]. After NEM treatment, the ATP-regenerating system was restored by adding additional creatine kinase, target RNA was added and the incubation was continued for the indicated time. OH^- denotes a base hydrolysis ladder.

5′ mismatch. Cleavage was similarly enhanced by the addition of a p1 mismatch to seven 3′ mismatches (49% cleavage versus 75% cleavage at 24 h) or to eight 3′ mismatches (21% versus 42% cleavage at 24 h). The finding that unpairing of the first base of the siRNA guide strand potentiated cleavage under single-turnover conditions suggests that a conformational change occurs in RISC during which the paired p1 base becomes unpaired before cleavage. Notably, p1 is often predicted to be unpaired for miRNAs bound to their targets[23–25].

For siRNAs that pair fully with their RNA targets, the scissile phosphate always lies between the target nucleotides that pair with siRNA bases 10 and 11 (refs. 2,9). Analysis at single-nucleotide resolution of the 5′ cleavage products generated by siRNAs with three, four or five 5′ mismatches (**Fig. 4d**) or six 3′ terminal mismatches (data not shown) revealed that the scissile phosphate on the target RNA remained the same, even when five 5′ nucleotides of the siRNA guide strand were mismatched with the target RNA (**Fig. 4d**). As discussed below, this result suggests that the identity of the scissile phosphate is a consequence of the structure of RISC, rather than being measured from the 5′ end of the helix formed between the siRNA and its RNA target.

Kinetic analysis of RISC catalysis

What role do nucleotides in the terminal regions of the siRNA guide strand play in directing RISC activity? Reduced pairing between an siRNA and its target might disrupt the binding of RISC to its target alternatively, mismatches might disrupt the structure, but not the affinity, of the siRNA-target interaction. Fully matched siRNAs are thought to form a 21-base pair, A-form helix with the target RNA[19,26], but do all parts of this helix contribute equally to target binding or do some regions provide only a catalytically permissive geometry? To distinguish between these possibilities, we analyzed the Michaelis-Menten kinetics of siRNA-directed target-RNA cleavage for a perfectly matched siRNA and for three siRNAs mismatched at their termini. siRNAs were assembled into RISC, diluted with reaction buffer to the desired RISC concentration and mixed with target RNA. For each siRNA, the initial velocity of reaction was determined at multiple substrate concentrations (**Supplementary Fig. 3** online), and K_m and k_{cat} were determined from a nonlinear least squares fit of substrate concentration versus initial velocity (**Fig. 5a**). By this assay, we estimate that the K_m of the *let-7* siRNA with complete complementarity to its target is ~8.4 nM (**Table 1**). We could not detect a difference in K_m, within error, between the fully paired siRNA and siRNA variants bearing three to five mismatches at their 3′ end or three mismatches at their 5′ end (**Fig. 5a** and **Table 1**). We note that for the mismatched siRNAs we used a higher than optimal enzyme concentration to detect cleavage. Therefore, our K_m measurements for the mismatched siRNAs represent an upper bound for the actual K_m values.

Although the K_m was unaltered for the *let-7* siRNA containing several terminal mismatches, the turnover number, k_{cat}, was decreased by terminal mismatches (**Table 1**). Three mismatches at the 5′ end of the siRNA halved the k_{cat}, whereas three 3′ mismatches decreased k_{cat} more than six-fold. The introduction of five 3′ mismatches did not increase the K_m, yet decreased k_{cat} >25-fold.

K_m reflects the binding strength of RISC

To estimate the contribution of binding to K_m, we used a competition assay that measures the ability of 2′-*O*-methyl oligonucleotides to inhibit target cleavage by RISC (**Fig. 5b**). Such a strategy has been used previously to analyze the mechanism of target destruction by antisense oligonucleotides that recruit RNase H[27]. We anticipated that 2′-*O*-methyl oligonucleotides would act as competitive inhibitors of RISC, because they bind to RISC containing complementary siRNA but not to RISC containing unrelated siRNA[21,28]. We designed 31-nt, 2′-*O*-methyl oligonucleotides as described[21], taking care to exclude sequences predicted to form stable internal structures. We chose 2′-*O*-methyl oligonucleotides because of their marked stability in *D. melanogaster* lysate and because they can be added to the reaction at high micromolar concentration.

Competition by 2′-*O*-methyl oligonucleotides and authentic RNA targets was quantitatively similar. We analyzed the reaction

© 2004 Nature Publishing Group http://www.nature.com/natstructmolbiol

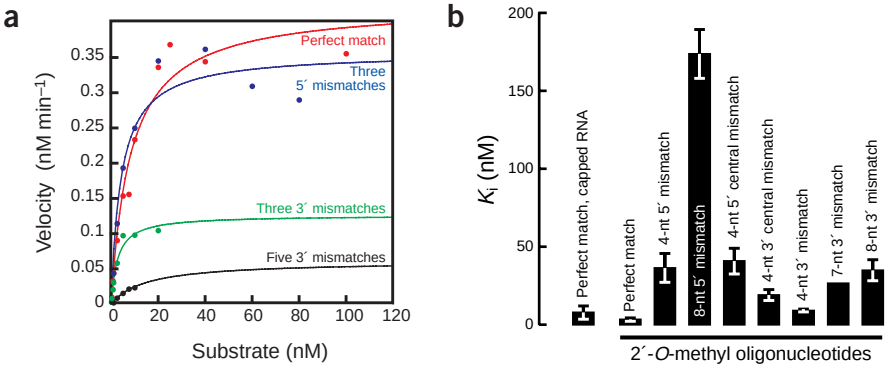

Figure 5 Michaelis-Menten and K_i analysis for matched and mismatched siRNAs reveal distinct contributions to binding and catalysis for the 5′, central and 3′ regions of the siRNA. (**a**) siRNA was assembled into RISC under standard *in vitro* RNAi conditions, and then diluted to achieve the desired RISC concentration. The initial rates of cleavage were determined for increasing concentrations of 5′ ^{32}P-cap-radiolabled target mRNA. Plot of initial velocity versus substrate concentration. K_m and V_{max} were determined by fitting the data to the Michaelis-Menten equation. See **Table 1** for analysis. Representative initial rate determinations appear in **Supplementary Figure 2** online. (**b**) K_i values were determined in competition assays using 2′-*O*-methyl oligonucleotides bearing 5′, central and 3′ mismatches to the siRNA guide strand. Representative data are presented in **Supplementary Figure 2** online, and a complete list of the 2′-*O*-methyl oligonucleotides used appears in **Supplementary Figure 3** online.

velocities of siRNA-directed cleavage of a ^{32}P-radiolabled target in the presence of increasing concentrations of unlabeled capped RNA target or a 31-nt 2′-*O*-methyl oligonucleotide corresponding to the region of the target containing the siRNA-binding site (**Fig. 5b**). Lineweaver-Burk analysis of the data confirms that 2′-*O*-methyl oligonucleotides act as competitive inhibitors of RISC (data not shown). These data were used to calculate K_i values for the perfectly matched RNA and 2′-*O*-methyl competitors. For the capped RNA competitor, the K_i was ~7.7 ± 4 nM (**Fig. 5b**), nearly identical to the K_m for this siRNA, 8.4 nM (**Table 1**). The K_i for the perfectly matched 2′-*O*-methyl competitor oligonucleotide was 3.2 ± 1 nM (**Fig. 5b**), essentially the same, within error, as that of the all-RNA competitor. We conclude that 2′-*O*-methyl oligonucleotides are good models for 5′-capped RNA targets and that the K_m for target cleavage by RISC is largely determined by the affinity (K_d) of RISC for its target RNA.

Although targets with more than five contiguous mismatches to either end of the siRNA are poor substrates for cleavage, they might nonetheless bind RISC and compete with the ^{32}P-radiolabeled target RNA. We used the 2′-*O*-methyl oligonucleotide competition assay to determine the K_i values for oligonucleotides containing as many as eight mismatches to the siRNA guide strand (**Fig. 5b**). 2′-*O*-methyl oligonucleotides with 3′ terminal mismatches to the siRNA were good competitors: a 4-nt mismatch with the 3′ end of the siRNA increased the K_i by only about three-fold (9.0 ± 0.9 nM) and an 8-nt mismatch with the 3′ end of the siRNA increased the K_i by about ten-fold (34.8 ± 7 nM). In contrast, mismatches with the 5′ end of the siRNA had a marked effect on binding. A 4-nt mismatch to the 5′ end of the siRNA increased the K_i ~12-fold (36.4 ± 9.2 nM) and an 8-nt mismatch to the 5′ end of the siRNA increased the K_i 53-fold (173 ± 16 nM). The differential effect on binding between 5′ and 3′ mismatches was maintained even at the center of the siRNA: a 2′-*O*-methyl oligonucleotide bearing four mismatches with siRNA nucleotides 11, 12, 13 and 14 (4-nt 3′ central mismatch, **Fig. 5b**) bound more tightly to RISC (that is, had a lower K_i) than an oligonucleotide with four mismatches to siRNA positions 7, 8, 9 and 10 (4-nt 5′ central mismatch, **Fig. 5b**).

DISCUSSION

RISC programmed with exogenous siRNA is an enzyme capable of multiple rounds of target cleavage. Our previous work has shown that cleavage of a target RNA by RISC does not require ATP[3,29]. The more detailed kinetic analysis presented here suggests that there are no ATP-assisted steps in either target recognition or cleavage by *D. melanogaster* RISC; we detect no difference in rate in the presence or absence of ATP for RNAi reactions analyzed under conditions of substrate excess at early time points (pre-steady state) or under conditions of enzyme excess where the reaction was essentially single-turnover. In contrast, the steady-state rate of cleavage under multiple-turnover conditions was enhanced four-fold by ATP. Our data suggest that release of the products of the RISC endonuclease is rate-determining under these conditions in the absence of ATP, but not in the presence of ATP. The most straightforward explanation for this finding is that an ATP-dependent RNA helicase facilitates the dissociation of the products of target cleavage from the RISC-bound

Table 1 Kinetic analysis of RISC

Mismatches and position	K_m (nM)	V_{max} (nM s^{-1})	[RISC] (nM)	k_{cat} (s^{-1})	k_{cat} K_m^{-1} (nM^{-1} s^{-1})	Fold change (k_{cat} K_m^{-1})
None	8.4 ± 1.6	0.0071	1	7.1×10^{-3}	8.4×10^{-4}	1.00
3-nt 3′	2.7 ± 0.6	0.0022	2	1.1×10^{-3}	3.8×10^{-4}	0.46
5-nt 3′	6.0 ± 1.8	0.0054	2	2.7×10^{-4}	4.5×10^{-5}	0.05
3-nt 5′	4.7 ± 1.3	0.0063	2	3.2×10^{-3}	6.7×10^{-4}	0.80
Reference enzymes	**K_m (nM)**			**k_{cat} (s^{-1})**	**k_{cat} K_m^{-1} (nM^{-1} s^{-1})**	**k_{cat} K_m^{-1} relative to RISC**
Urease	2.5×10^7			1×10^4	4.0×10^{-4}	0.47
Fumarase	5.0×10^3			8×10^2	1.6×10^{-1}	190
Catalase	2.5×10^7			1×10^7	4.0×10^{-1}	8,940
RNase H1	3.8×10^1			5×10^2	1.3×10^{-3}	0.03

Summary of kinetic data from the analysis in **Figure 5a**. For comparison, the K_m and k_{cat} values of four well-studied protein enzymes, urease[44], fumarase[44], catalase[44] and RNase H1 (ref. 45), are provided. K_m ± error of fit is reported.

© 2004 Nature Publishing Group http://www.nature.com/natstructmolbiol

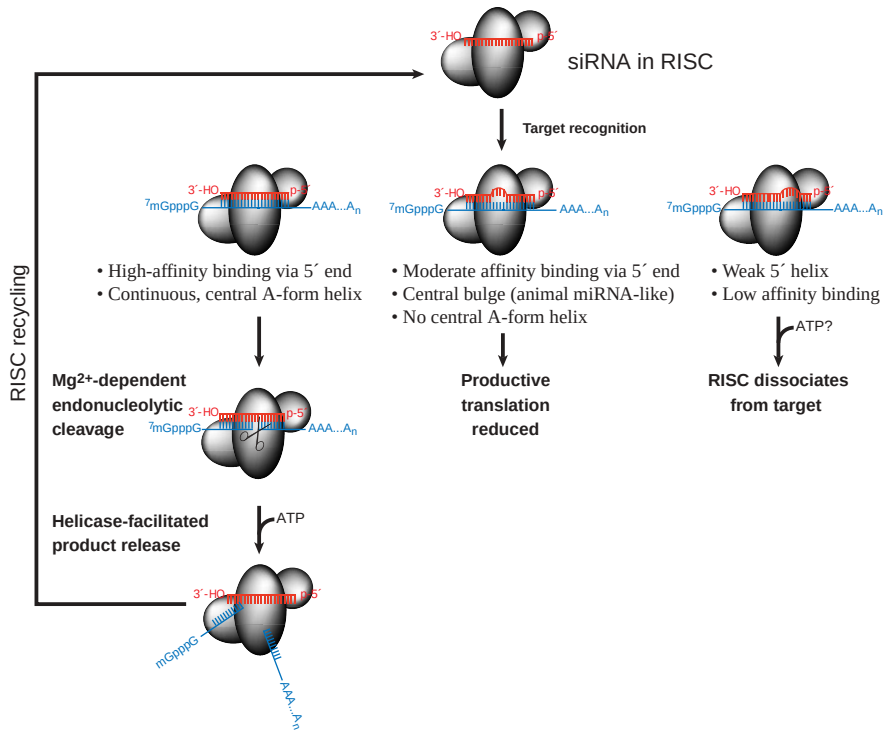

Figure 6 A model for the cycle of RISC assembly, target recognition, catalysis and recycling.

siRNA. The involvement of such an ATP-dependent helicase in RNAi *in vivo* may explain why siRNAs can be active within a broad range of GC content[30].

In the presence of ATP, siRNA-programmed *D. melanogaster* RISC is a classical Michaelis-Menten enzyme. The guide strand of the siRNA studied here has the sequence of *let-7*, an endogenous miRNA. *In vivo*, *let-7* is not thought to direct mRNA cleavage, but rather is believed to repress productive translation of its mRNA targets. Nonetheless, the *let-7* siRNA is among the most potent of the siRNAs we have studied *in vitro* and provides a good model for effective siRNA in general. With a k_{cat} of ~7×10^{-3} s^{-1}, the *let-7* siRNA-programmed RISC was slow compared with enzymes with small molecule substrates (**Table 1**). The K_m for this RISC was ~8 nM. Enzymes typically have K_m values between 1- and 100-fold greater than the physiological concentrations of their substrates[31]. Our data suggest that RISC is no exception: individual abundant mRNA species are present in eukaryotic cells at high picomolar or low nanomolar concentration. The K_m of RISC is probably determined primarily by the strength of its interaction with the target RNA, because the K_m is nearly identical to the K_i of a noncleavable 2′-*O*-methyl oligonucleotide inhibitor.

Recently, Tuschl and colleagues have measured the kinetic parameters of target RNA cleavage by human RISC[32]. In that study, the minimal active human RISC was highly purified; in this study, *D. melanogaster* RISC activity was measured for the unpurified, intact holo-RISC, believed to be an 80S multiprotein complex[33]. Different siRNAs were used in the two studies. Nonetheless, the K_m and k_{cat} values reported here and for the minimal human RISC are markedly similar: the K_m was 2.7–8.4 nM and the k_{cat} was 7.1×10^{-3} s^{-1} for the *let-7* siRNA-programmed *D. melanogaster* holo-RISC versus a K_m of 1.1–2.3 nM and a k_{cat} of 1.7×10^{-2} s^{-1} for a different siRNA in minimal human RISC. As in this study, Tuschl and colleagues also observed a pre-steady-state burst in the absence of ATP, consistent with the idea that product release is ATP-assisted *in vivo*.

The ratio of k_{cat} to K_m is a classical measure of enzyme efficiency and corresponds to the second-order rate constant for the reaction when the concentration of substrate is much less than the K_m. For the *let-7* programmed RISC, k_{cat} K_m^{-1} equals ~8.4×10^5 M^{-1} s^{-1} (~8.4×10^{-4} nM^{-1} s^{-1}), a value far slower than the expected rate of collision of RISC with mRNA, $\geq 10^7$ M^{-1} s^{-1}. What then limits the rate of catalysis by RISC? Perhaps cleavage by RISC is constrained by the rate of conformational changes required for formation of the enzyme–substrate complex or by subsequent conformational rearrangements required for catalysis. Future studies will be needed to determine if siRNAs can be designed that substantially improve either the k_{cat} or K_m of RISC without compromising specificity.

Although siRNAs are typically envisioned to bind their target RNAs through 19–21 complementary base pairs, we find that the 5′, central and 3′ regions of the siRNA make distinct contributions to binding and catalysis (**Fig. 6**). Measurements of K_m and K_i suggest that the 5′ nucleotides of the siRNA contribute more to target binding than do the 3′ nucleotides. At least for the siRNA examined here, the first three and the last five nucleotides of a 21-nt siRNA contribute little to binding. If the K_d of RISC bound to its target RNA is essentially its K_m, ~8 nM, then the free energy ($\Delta G° = -RT \ln K_d$) of the *let-7*-programmed RISC-target interaction is about –11 kcal mol^{-1}, considerably less than the –35 kcal mol^{-1} (K_d ~10^{-29}) predicted (http://ozone2.chem.wayne.edu/Hyther/hytherm1main.html) for the *let-7* RNA bound to a fully complementary RNA in 100 mM K^+ and 1.2 mM Mg^{2+} at 25 °C. Why does RISC seem to discard so much potential binding energy? Perhaps by binding less tightly to its target, an siRNA in RISC gains the ability to discriminate between well matched and poorly matched targets, but only for bases in the 5′ region of the siRNA guide strand.

Mismatches between the central and 3′ regions of an siRNA and its target RNA reduce k_{cat} far more than mismatches at the 5′ end of the siRNA. These results fit well with recent findings by Doench and Sharp that translational repression by siRNA, designed to act like animal miRNA, is markedly disrupted by mismatches with the 5′ end of the siRNA, but not with similar mismatches at the 3′ end[18]. These authors propose that miRNA binding is mediated primarily by nucleotides at the 5′ end of the small RNA. In fact, complementarity between the 5′ end of miRNAs and their targets has been required by all computational approaches for predicting animal miRNA targets[16,23,25,34]. Our finding that central and 3′ siRNA sequences must pair with the target sequence for effective target cleavage but not for target binding reinforces this view; both central and 3′ miRNA sequences are usually mismatched with their binding sites in their natural targets[35–41].

Formation of a contiguous A-form helix surrounding the scissile phosphate of the target mRNA has been proposed to be a quality control step for RISC-mediated target cleavage[19]. We find that RISC can direct cleavage when the siRNA is paired with the target RNA only at positions 2–12 of the guide strand, corresponding to one complete turn of an RNA-RNA helix. This region of the siRNA includes

© 2004 Nature Publishing Group http://www.nature.com/natstructmolbiol

nucleotides 2–8, which seem to be critical for miRNA recognition of mRNAs targeted for translational repression, plus two nucleotides flanking either side of the scissile phosphate. Our finding that unpairing the first nucleotide of the guide strand enhances the activity of siRNAs with seven, eight or nine 3′ mismatches to the RNA target is notable, as many miRNAs do not pair with their targets at this position. Furthermore, such pairing resembles that reported by Linsley and colleagues for siRNA-directed off-target effects in cultured mammalian cells[14].

The requirement for a full turn of a helix may reflect a mechanism of 'quality control' by RISC. Because RISC can apparently assemble on any siRNA sequence, it must use the structure of the siRNA paired to its target to determine whether or not to cleave. Despite the apparent surveillance of the structure of the siRNA-target pair, the identity of the scissile phosphate is unaltered by extensive mismatch between the 5′ end of the siRNA and its target. Yet the scissile phosphate is determined by its distance from the 5′ end of the siRNA guide strand[2,9]. The simplest explanation for our findings is that the scissile phosphate is identified by a protein loaded onto the siRNA during RISC assembly, that is, before the encounter of the RISC with its target RNA.

The remarkable tolerance of RISC for mismatches between the siRNA and its targets—up to nine contiguous 3′ nucleotides—implies that a large number of off-target genes should be expected for many siRNA sequences when RISC is present in excess over its RNA targets. However, RISC with extensive mismatches between the siRNA and target is quite slow to cleave, so off-target effects may be minimized by keeping the amount of RISC as low as possible. As our understanding of the molecular basis of siRNA-directed gene silencing grows, we anticipate that siRNA will be able to be designed to balance the competing demands of siRNA efficacy and specificity.

METHODS

General methods. *D. melanogaster* embryo lysate, siRNA labeling with polynucleotide kinase (New England Biolabs), target RNA preparation and labeling with guanylyl transferase were carried out as described[20,42], and the forward primer sequence for 379-nt target mRNA was 5′-CGC TAA TAC GAC TCA CTA TAG CAG TTG GCG CCG CGA ACG A-3′, and 5′-GCG TAA TAC GAC TCA CTA TAG TCA CAT CTC ATC TAC CTC C-3′ for the 182-nt target. Reverse primers used to generate fully matched and mismatched target RNAs were: 5′-CCC ATT TAG GTG ACA CTA TAG ATT TAC ATC GCG TTG AGT GTA GAA CGG TTG TAT AAA AGG TTG AGG TAG TAG GTT GTA TAG TGA AGA GAG GAG TTC ATG ATC AGT G-3′ (perfect match to let-7); 5′-CCC ATT TAG GTG ACA CTA TAG ATT TAC ATC GCG TTG AGT GTA GAA CGG TTG TAT AAA AGG TTG AGG TAG TAG GTT CAT GCA GGA AGA GAG GAG TTC ATG ATC AGT G-3′ (7-nt 3′ mismatch); 5′-CCC ATT TAG GTG ACA CTA TAG ATT TAC ATC GCG TTG AGT GTA GAA CGG TTG TAT AAA AGG TTG AGG TAG TAG GTA CAU GCA GGA AGA GAG GAG TTC ATG ATC AGT G-3′ (8-nt 3′ mismatch); 5′-CCC ATT TAG GTG ACA CTA TAG ATT TAC ATC GCG TTG AGT GTA GAA CGG TTG TAT AAA AGG TTG AGG TAG TAG GAA CAT GCA GGA AGA GAG GAG TTC ATG ATC AGT G-3′ (9-nt 3′ mismatch); 5′-CCC ATT TAG GTG ACA CTA TAG ATT TAC ATC GCG TTG AGT GTA GAA CGG TTG TAT AAA AGG TAC TCC ATC TAG GTT GTA TAG TGA AGA GAG GAG TTC ATG ATC AGT G-3′ (8-nt 5′ mismatch); 5′-CCC ATT TAG GTG ACA CTA TAG ATT TAC ATC GCG TTG AGT GTA GAA CGG TTG TAT AAA AGG TAC TCG TAG TAG GTT GTA TAG TGA AGA GAG GAG TTC ATG ATC AGT G-3′ (4-nt 5′ mismatch). The lengths of the target sequences were 613 nt (**Figs. 1–3** and **5a** and **Supplementary Figures 1** and **2** online); 379 nt (**Figs. 4a–c** and **5b** and **Supplementary Figure 2** online); and 182 nt (**Fig. 4d**). All siRNAs were deprotected according to the manufacturer's protocol (Dharmacon), 5′-radiolabeled where appropriate, and then gel-purified on 15% (w/v) denaturing PAGE. 2′-*O*-methyl oligonucleotides were from Dharmacon. siRNA strands were annealed at high concentrations and serially diluted into lysis buffer (30 nM HEPES, pH 7.4, 100 mM KOAc, and 2 mM $MgCl_2$). Gels were dried and imaged as described[22]. Images were analyzed using Image Gauge 4.1 (Fuji). Initial rates were determined by linear regression using Excel X (Microsoft) or IgorPro 5.01 (Wavemetrics). Kaleidagraph 3.6.2 (Synergy Software) was used to determine K_m and K_i by global fitting to the equations: $V = (V_{max} \times S)\,(K_m + S)^{-1}$ and $V = (V_{max} \times K_{i(app)})\,(K_{i(app)} + I)^{-1}$, where V is velocity, S is target RNA concentration, and I is the concentration of 2′-*O*-methyl oligonucleotide competitor. K_i was calculated by correcting $K_{i(app)}$ by the K_m and substrate concentration, $K_i = K_{i(app)}\,(1 + (S\,K_m^{-1}))^{-1}$.

ATP depletion and NEM inhibition. RNAi reactions using *D. melanogaster* embryo lysate were done as described[42]. To compare –ATP and +ATP conditions, samples were treated with 10 mM NEM (Pierce) for 10 min at 4 °C, and then the NEM was quenched with 11 mM DTT. For ATP depletion (–ATP), 1 unit of hexokinase and 20 mM (final concentration) glucose were added and the incubation continued for 30 min at 25 °C. For +ATP reactions, 0.05 mg ml^{-1} (final concentration) creatine kinase and one-tenth volume H_2O were substituted for hexokinase and glucose, respectively. The addition of fresh creatine kinase after NEM treatment did not rescue the defect in RISC assembly, but did restore ATP to high levels[3]. ATP levels were measured using an ATP assay kit (Sigma) and a PhL luminometer (Mediators Diagnostika).

Note: Supplementary information is available on the Nature Structural & Molecular Biology website.

ACKNOWLEDGMENTS
We thank J. McLachlan for maintaining our fly colony, and members of the Zamore lab, S. Blacklow, T. Carruthers and D. Turner for encouragement, helpful discussions and comments on the manuscript. P.D.Z. is a Pew scholar in the biomedical sciences and a W.M. Keck Foundation young scholar in medical research. This work was supported in part by grants from the US National Institutes of Health to P.D.Z. (GM62862-01 and GM65236-01).

COMPETING INTERESTS STATEMENT
The authors declare competing financial interests (see *Nature Structural & Molecular Biology* website for details).

Received 31 March; accepted 12 May 2004
Published online at http://www.nature.com/nsmb/

1. Fire, A. *et al.* Potent and specific genetic interference by double-stranded RNA in Caenorhabditis elegans. *Nature* **391**, 806–811 (1998).
2. Elbashir, S.M., Lendeckel, W. & Tuschl, T. RNA interference is mediated by 21- and 22-nucleotide RNAs. *Genes Dev.* **15**, 188–200 (2001).
3. Nykänen, A., Haley, B. & Zamore, P.D. ATP requirements and small interfering RNA structure in the RNA interference pathway. *Cell* **107**, 309–321 (2001).
4. Martinez, J., Patkaniowska, A., Urlaub, H., Lührmann, R. & Tuschl, T. Single-stranded antisense siRNA guide target RNA cleavage in RNAi. *Cell* **110**, 563–574 (2002).
5. Hammond, S.M., Bernstein, E., Beach, D. & Hannon, G.J. An RNA-directed nuclease mediates post-transcriptional gene silencing in *Drosophila* cells. *Nature* **404**, 293–296 (2000).
6. Hannon, G.J. & Zamore, P.D. Small RNAs, big biology and biochemical studies of RNA interference. In *RNAi: A Guide To Gene Silencing* (ed. Hannon, G.J.) 87–108 (Cold Spring Harbor Laboratory Press, Cold Spring Harbor, NY, 2003).
7. Elbashir, S.M. *et al.* Duplexes of 21-nucleotide RNAs mediate RNA interference in cultured mammalian cells. *Nature* **411**, 494–498 (2001).
8. Amarzguioui, M., Holen, T., Babaie, E. & Prydz, H. Tolerance for mutations and chemical modifications in a siRNA. *Nucleic Acids Res.* **31**, 589–595 (2003).
9. Elbashir, S.M., Martinez, J., Patkaniowska, A., Lendeckel, W. & Tuschl, T. Functional anatomy of siRNAs for mediating efficient RNAi in *Drosophila melanogaster* embryo lysate. *EMBO J.* **20**, 6877–6888 (2001).
10. Holen, T., Amarzguioui, M., Babaie, E. & Prydz, H. Similar behaviour of single-strand and double-strand siRNAs suggests they act through a common RNAi pathway. *Nucleic Acids Res.* **31**, 2401–2407 (2003).
11. Tang, G., Reinhart, B.J., Bartel, D.P. & Zamore, P.D. A biochemical framework for RNA silencing in plants. *Genes Dev.* **17**, 49–63 (2003).
12. Phipps, K.M., Martinez, A., Lu, J., Heinz, B.A. & Zhao, G. Small interfering RNA molecules as potential anti-human rhinovirus agents: *in vitro* potency, specificity, and mechanism. *Antiviral Res.* **61**, 49–55 (2004).
13. Ding, H. *et al.* Selective silencing by RNAi of a dominant allele that causes amyotrophic lateral sclerosis. *Aging Cell* **2**, 209–217 (2003).
14. Jackson, A.L. *et al.* Expression profiling reveals off-target gene regulation by RNAi. *Nat. Biotechnol.* **21**, 635–637 (2003).
15. Bartel, D.P. MicroRNAs: genomics, biogenesis, mechanism, and function. *Cell* **116**, 281–297 (2004).
16. Rajewsky, N. & Socci, N.D. Computational identification of microRNA targets. *Dev. Biol.* **267**, 529–535 (2004).

© 2004 Nature Publishing Group http://www.nature.com/natstructmolbiol

17. Lai, E.C. Micro RNAs are complementary to 3′ UTR sequence motifs that mediate negative post-transcriptional regulation. *Nat. Genet.* **30**, 363–364 (2002).
18. Doench, J.G. & Sharp, P.A. Specificity of microRNA target selection in translational repression. *Genes Dev.* **18**, 504–511 (2004).
19. Chiu, Y.L. & Rana, T.M. siRNA function in RNAi: a chemical modification analysis. *RNA* **9**, 1034–1048 (2003).
20. Hutvágner, G. & Zamore, P.D. A microRNA in a multiple-turnover RNAi enzyme complex. *Science* **297**, 2056–2060 (2002).
21. Hutvágner, G., Simard, M.J., Mello, C.C. & Zamore, P.D. Sequence-specific inhibition of small RNA function. *PLoS Biol.* **2**, 1–11 (2004).
22. Schwarz, D.S. *et al.* Asymmetry in the assembly of the RNAi enzyme complex. *Cell* **115**, 199–208 (2003).
23. Lewis, B., Shih, I., Jones-Rhoades, M., Bartel, D. & Burge, C. Prediction of mammalian microRNA targets. *Cell* **115**, 787–798 (2003).
24. Rhoades, M.W. *et al.* Prediction of plant microRNA targets. *Cell* **110**, 513–520 (2002).
25. Stark, A., Brennecke, J., Russel, R. & Cohen, S. Identification of *Drosophila* microRNA targets. *PLoS Biol.* **1**, 1–13 (2003).
26. Chiu, Y.-L. & Rana, T.M. RNAi in human cells: basic structural and functional features of small interfering RNA. *Molecular Cell* **10**, 549–561 (2002).
27. Lima, W.F. & Crooke, S.T. Binding affinity and specificity of *Escherichia coli* RNase H1: impact on the kinetics of catalysis of antisense oligonucleotide-RNA hybrids. *Biochemistry* **36**, 390–398 (1997).
28. Meister, G., Landthaler, M., Dorsett, Y. & Tuschl, T. Sequence-specific inhibition of microRNA- and siRNA-induced RNA silencing. *RNA* **10**, 544–550 (2004).
29. Tomari, Y. *et al.* RISC assembly defects in the *Drosophila* RNAi mutant armitage. *Cell* **116**, 831–841 (2004).
30. Reynolds, A. *et al.* Rational siRNA design for RNA interference. *Nat. Biotechnol.* **22**, 326–330 (2004).
31. Stryer, L. *Biochemistry.* (W. H. Freeman and Company, San Francisco; 1981).
32. Martinez, J. & Tuschl, T. RISC is a 5′ phosphomonoester-producing RNA endonuclease. *Genes Dev.* **18**, 975–980 (2004).
33. Pham, J.W., Pellino, J.L., Lee, Y.S., Carthew, R.W. & Sontheimer, E.J. A Dicer-2-dependent 80S complex cleaves targeted mRNAs during RNAi in *Drosophila*. *Cell* **117**, 83-94 (2004).
34. Enright, A. *et al.* MicroRNA targets in *Drosophila*. *Genome Biol.* **5**, R1 (2003).
35. Lee, R.C., Feinbaum, R.L. & Ambros, V. The *C. elegans* heterochronic gene *lin-4* encodes small RNAs with antisense complementarity to *lin-14*. *Cell* **75**, 843–854. (1993).
36. Reinhart, B.J. *et al.* The 21-nucleotide *let-7* RNA regulates developmental timing in *Caenorhabditis elegans*. *Nature* **403**, 901–906. (2000).
37. Brennecke, J., Hipfner, D.R., Stark, A., Russell, R.B. & Cohen, S.M. *bantam* encodes a developmentally regulated microRNA that controls cell proliferation and regulates the proapoptotic gene *hid* in *Drosophila*. *Cell* **113**, 25–36 (2003).
38. Abrahante, J.E. *et al.* The *Caenorhabditis elegans hunchback*-like gene *lin-57/hbl-1* controls developmental timing and is regulated by microRNAs. *Dev. Cell* **4**, 625–637 (2003).
39. Vella, M., Choi, E., Lin, S., Reinert, K. & Slack, F. The *C. elegans* microRNA *let-7* binds to imperfect *let-7* complementary sites from the *lin-41* 3′UTR. *Genes Dev.* **18**, 132–137 (2004).
40. Xu, P., Vernooy, S.Y., Guo, M. & Hay, B.A. The *Drosophila* microRNA miR-14 suppresses cell death and is required for normal fat metabolism. *Curr. Biol.* **13**, 790–795 (2003).
41. Johnston, R.J. & Hobert, O. A microRNA controlling left/right neuronal asymmetry in *Caenorhabditis elegans*. *Nature* **426**, 845–849 (2003).
42. Haley, B., Tang, G. & Zamore, P.D. *In vitro* analysis of RNA interference in *Drosophila melanogaster*. *Methods* **30**, 330–336 (2003).
43. Schwarz, D.S., Tomari, Y. & Zamore, P.D. The RNA-induced silencing complex is a Mg^{2+}-dependent endonuclease. *Curr. Biol.* **14**, 787–791 (2004).
44. Voet, D. & Voet, J.G. *Biochemistry.* (John Wiley & Sons, Hoboken, NJ; 2004).
45. Wu, H., Lima, W.F. & Crooke, S.T. Investigating the structure of human RNase H1 by site-directed mutagenesis. *J. Biol. Chem.* **276**, 23547–23553. (2001).

© 2004 Nature Publishing Group http://www.nature.com/natstructmolbiol